Stability analysis of dynamic ratcheting in elastoplastic systems

Noël Challamel* and Christophe Lanos†
Laboratoire de Génie Civil et Génie Mécanique, INSA de Rennes, 20 Avenue des Buttes de Coësmes, 35043 Rennes Cedex, France

Abdelaziz Hammouda‡ and Bachir Redjel§
BP 25 SIDI-AMAR, 23220 Annaba, Algerie

(Received 6 July 2006; published 6 February 2007)

This paper deals with the stability and the dynamics of a harmonically excited elastic perfectly plastic asymmetrical oscillator. The hysteretical system is written as a nonsmooth, forced autonomous system. The dimension of the phase space can be reduced using adapted variables. It is shown that asymmetry of boundary conditions (forcing term) and material asymmetry lead to an equivalent system for this simple structural case. The forced vibration of such an oscillator is treated by a numerical approach by using time locating techniques. Stability of the limit cycles is analytically investigated with a perturbation approach. The boundary between elastoplastic shakedown and dynamic ratcheting is given in closed form. It is shown that the divergence rate is strongly correlated to the internal asymmetry of the oscillator.

DOI: 10.1103/PhysRevE.75.026204 PACS number(s): 05.45.−a, 83.85.Vb, 62.20.Fe, 46.70.−p

I. INTRODUCTION

In seismic design, hysteretic loops of structural elements may exhibit highly asymmetric shape due to asymmetry in geometry, boundary conditions, or material properties. This asymmetric feature may be closely connected to the concept of ratcheting phenomenon, which is characterized by an unbounded evolution of the state variables [1]. Such a strain (or displacement) accumulation can be unacceptable for the safety or reliability of the component behavior. There is much literature devoted to this phenomenon in the field of mechanics of materials, especially when plasticity is predominant [2], but there is also much literature devoted to this phenomenon in physics of molecular motors. Inspired by the Smoluchowski–Feynman ratchet [3], a variety of mechanisms of molecular motors has been suggested [4–10]. The fundamental condition for the ratchet phenomenon to occur is that certain symmetries associated with constitutive law or time variables are broken. These are the cases of the motion of a particle in a spatially periodic potential with an asymmetric profile [7], of the dynamical behavior of a moving system due to asymmetric dependence of the friction [8], or of the modeling of an impact system with a drift [11]. The dynamics analysis of the elastoplastic ratchet has not been extensively studied, a recent paper [12] being probably an exception.

This paper examines the condition to be fulfilled by a simple asymmetrical elastic perfect oscillator to exhibit dynamic ratcheting. The paper also presents some fundamental phenomena associated with the theory of dynamic shakedown of elastoplastic structures. Shakedown can be defined as the capability for the oscillator to converge toward a stationary elastic regime (stationary regime without plastic phases). This property is very important for the structural system to be guaranteed, in order to achieve reliable engineering design (the reader should refer to [13] for an extensive description of this problem in quasistatic analysis). It will be shown that asymmetry of boundary conditions and material asymmetry lead to an equivalent system for this simple structural case. Stability of the periodic evolutions is investigated using classical tools of nonsmooth dynamics (see, for instance, [14]).

There have been numerous studies on the forced response of elastoplastic oscillators using a bilinear hysteretic model (also called linear kinematic hardening rule). Jacobsen [15] and Tanabashi [16] are among the earlier investigators studying the forced vibration response of yielding oscillators to simple pulses and square waves. Caughey [17] obtained an approximation of the steady-state response of the undamped bilinear hysteretic oscillator subjected to harmonic pulsation. Caughey [17] used the method of slowly varying parameters (based on the works of Kryloff–Bogoliuboff) to approximate the response and to investigate the stability of the postulated periodic evolutions. One of the main results of Caughey's reference study is that the steady-state response of this oscillator was stable for all the involved parameters. Jennings [18] or Iwan [19] generalized the results of Caughey [17] by considering more complex hysteretic models and by adding some damping. The first considers Ramberg–Osgood's model, whereas the second studies a particular hysteretic model called the double bilinear hysteretic model. More recently, Capecchi [20] studied Bouc's hysteresis model. It is not the purpose of this paper to enumerate all hysteresis models and their dynamics properties. The important point is that most of these studies use mainly approximate analytical techniques such as an averaging method [17–19], harmonic balance method [21], or by combining the Fourier transform and harmonic balance techniques [20]. The latter is probably one of the most efficient. However, the accuracy of the results depends, like all harmonic balance techniques, on the number of harmonics included. These problems become more prominent if the response contains sharp spikes (i.e., due to the sharp change in the restoring force at the elastic-

*Electronic address: noel.challamel@insa-rennes.fr
†Electronic address: christophe.lanos@univ-rennes1.fr
‡Electronic address: hamouda-az@yahoo.fr
§Electronic address: bredjel@yahoo.fr

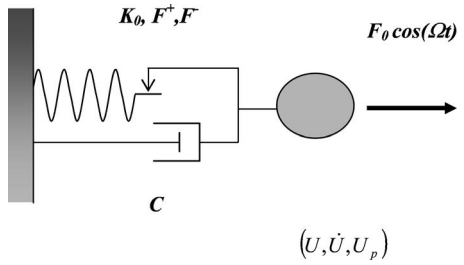

FIG. 1. Description of the elastic perfectly plastic oscillator.

plastic boundary) when a large number of harmonics need to be retained [22]. In the present paper, it is shown that the dynamics of the elastoplastic oscillator is a forced piecewise linear system. The dynamics is computed using the time locating techniques, as initiated by Masri [23] for impact dampers. The stability analysis is carried out by using a perturbation approach, first applied to impact dampers [24]. Due to the nonsmooth nonlinearities, the stability of the periodic solution is determined by investigating the asymptotic behavior of perturbations to the steady-state periodic solution, as the usual method involving the classical Floquet theory is not applicable to such a nonsmooth system. This method, also called the method of error propagation [22], needs the accurate knowledge of the number of junctions to be encountered during one period. A similar method was applied by Miller and Butler [25] or Capecchi [26] to the undamped elastoplastic oscillator. The damped elastoplastic oscillator was studied by Masri [27], who investigated the exact steady-state motion by using the piecewise linear properties of the nonsmooth dynamical system. Masri [27] extended the pioneering work of Iwan [28] who also determined the exact steady-state motion of the undamped system. Coman [29] questioned the boundedness of trajectories of the damped elastoplastic oscillator. Dynamics of the damped forced elastoplastic oscillator has been recently considered by Liu and Huang [30] and Challamel and Gilles [31], who have obtained a closed-form solution of the exact steady-state motion. Challamel and Gilles [31] have also shown the asymptotic stability of the symmetrical periodic orbit with the presented perturbation approach. The dynamics of the asymmetric Bouc–Wen model is numerically studied by Song and der Kiureghian [32]. Dynamic ratcheting is investigated by Ahn *et al.* [12], who studied a symmetric elastoplastic oscillator subjected to a dual-frequency sinusoidal excitation.

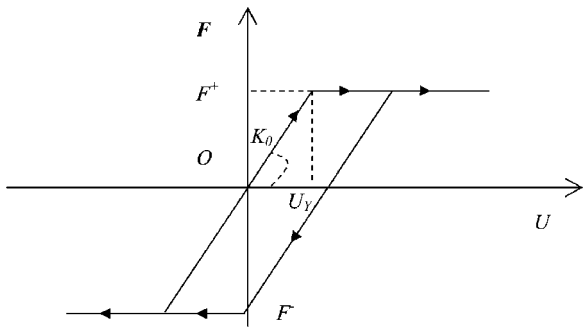

FIG. 2. Plastic incremental law for the inelastic spring; asymmetrical case: $|F^+| \neq |F^-|$.

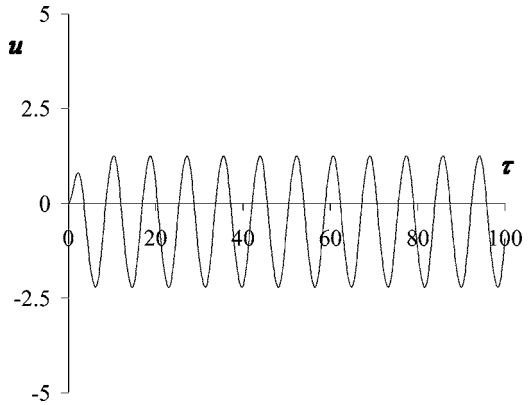

FIG. 3. Alternating plasticity, no ratcheting effect: $\zeta=0.1$; $f_0=0.8$; $\omega=0.75$; $\varepsilon=0-u_0=u_{p0}=\dot{u}_0=0$.

It is interesting to notice that dynamics of elastoplastic oscillators, dynamics of friction oscillators, or dynamics of impact dampers are finally closely connected by similar analysis techniques due to their nonsmooth nature. The friction problem is probably the first one to have been investigated using piecewise elastic solutions [33,34]. The methodology is exactly the same as for piecewise linear elastic oscillators [35]. Recent theoretical contributions to the stability analysis of these periodically forced piecewise linear oscillators are those of Wiercigroch [36], Awrejcewicz and Lamarque [14], Ji and Leung [37], Luo and Chen [38], or Csernak and Stépàn [39].

In this paper, the presented perturbation method is applied to the harmonically excited elastic perfectly plastic oscillator. In the first part, the dynamic hysteretic system is written as a nonsmooth, forced autonomous system. It is shown that the dimension of the phase space can be reduced using adapted variables. The forced vibration of such an oscillator is treated by a numerical approach using the time locating technique. The stability of the limit cycles obtained for a certain range of structural parameters (damping, force intensity, excitation frequency, and asymmetric parameter) is then analytically investigated.

II. EQUATIONS OF MOTION

Let us consider the simple system shown in Fig. 1. A mass

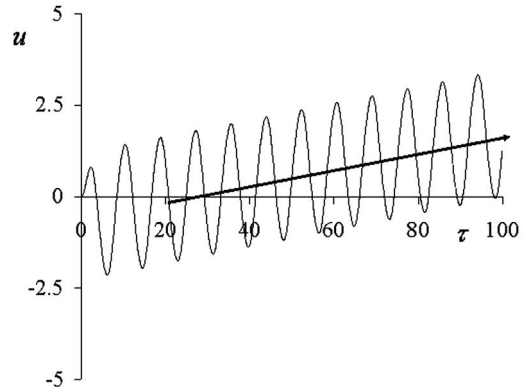

FIG. 4. Ratcheting: $\zeta=0.1$; $f_0=0.8$; $\omega=0.75$; $\varepsilon=0.05-u_0=u_{p0}=\dot{u}_0=0$.

M is attached to a viscous elastoplastic spring. The inelastic system is externally excited by a harmonic force $F(t)$ defined by the intensity F_0 and angular frequency Ω. t is the time and a superposed dot represents a time differentiation. This oscillator is characterized by the displacement U, displacement rate $\dot{U}$, and a plastic internal variable, chosen as the plastic displacement U_p. The plastic incremental law is illustrated in Fig. 2. This is a simple, asymmetrical, elastoplastic perfect law which depends on three parameters, i.e., the elastic stiffness K_0, the maximum force F^+, and the minimum force F^-. U_Y is an elastic characteristic displacement $(U_Y=F^+/K_0)$. The damping coefficient is denoted by C (positive parameter).

Two dynamic states can be distinguished. These two states correspond to a reversible state $\hat{E}$ (or elastic state) and an irreversible state $\hat{P}$ (or plastic state) associated with plastic displacement evolution. This plastic state $\hat{P}$ can be decomposed into two states $\hat{P}^+$ and $\hat{P}^-$, depending on the sign of the elastic displacement $U-U_p$. The equation of motion of the damped elastoplastic oscillator can be written as

$$\left|\begin{array}{ll} \hat{E} \text{ state: } M\ddot{U}+C\dot{U}+K_0(U-U_p)=F(t);\ \dot{U}_p=0 & \\ \hat{P}^+ \text{ state: } M\ddot{U}+C\dot{U}+F^+=F(t);\ \dot{U}_p=\dot{U} & \text{with } F(t)=F_0\cos\Omega t. \\ \hat{P}^- \text{ state: } M\ddot{U}+C\dot{U}+F^-=F(t);\ \dot{U}_p=\dot{U} & \end{array}\right. \tag{1}$$

Such oscillators potentially have asymmetrical strength (if $|F^+|\neq|F^-|$), but the forcing term is symmetrical in this case. Each state is defined from a partition of the phase space $(U,\dot{U},U_p)$,

$$\left|\begin{array}{l} \hat{E} \text{ state: } \{F^-<K_0(U-U_p)<F^+\} \text{ or } \{[K_0(U-U_p)=F^+] \text{ and } [\dot{U}(U-U_p)\leq 0]\} \\ \text{or } \{[K_0(U-U_p)=F^-] \text{ and } [\dot{U}(U-U_p)\leq 0]\} \\ \hat{P}^+ \text{ state: } [K_0(U-U_p)=F^+] \text{ and } \dot{U}\geq 0 \\ \hat{P}^- \text{ state: } [K_0(U-U_p)=F^-] \text{ and } \dot{U}\leq 0 \end{array}\right. . \tag{2}$$

This is clearly a piecewise linear oscillator and a nonsmooth system. This system is very close to the one considered by Wagg [40], who studied a nonlinear elastic oscillator with asymmetric thresholds (a bilinear elastic oscillator). However, in the present case (an elastoplastic oscillator), no period doubling bifurcation has been observed for positive damping values.

The dimensionless phase variables are introduced as follows:

$$(u,\dot{u},u_p)=\left(\frac{U}{U_Y},\frac{\dot{U}}{U_Y},\frac{U_p}{U_Y}\right). \tag{3}$$

The time constant of the dynamical system is introduced as

$$t^*=\sqrt{\frac{M}{K_0}}. \tag{4}$$

New temporal derivatives can be calculated with respect to the dimensionless time parameter τ,

$$\tau=\frac{t}{t^*}. \tag{5}$$

It means that the dot now represents a time differentiation with respect to dimensionless variable τ. The dimensionless parameter ε can be introduced in order to quantify the asymmetric strength,

$$\frac{F^-}{F^+}=-1-\varepsilon \quad \text{with } \varepsilon>0. \tag{6}$$

ε is assumed to be positive such that the strength in compression is greater than the one in tension. Moreover, the dimension of the phase space can be reduced using the elastic displacement variable

$$v=u-u_p. \tag{7}$$

The new phase space is then reduced to $(v,\dot{u})$. This is an important property of this perfectly plastic oscillator. Such a reduction of the dimension of the phase space would not be possible for the kinematic hardening plastic oscillator, for instance. This property significantly simplifies the calculations for the investigations of the steady-state motion and for the stability analysis. It can be remarked that the elastic displacement is nothing else than the constitutive force for the dimensionless dynamical

system. This reduced phase space was also used by Capecchi [26], Coman [29], and Challamel [41]. Thus, the new equivalent dynamical system is now given by

$$\left|\begin{array}{l} \hat{E} \text{ state: } \ddot{u}+2\zeta\dot{u}+v=f_0\cos\omega\tau;\ \dot{v}=\dot{u} \\ \hat{P}^{+} \text{ state: } \ddot{u}+2\zeta\dot{u}+1=f_0\cos\omega\tau;\ \dot{v}=0 \\ \hat{P}^{-} \text{ state: } \ddot{u}+2\zeta\dot{u}-(1+\varepsilon)=f_0\cos\omega\tau;\ \dot{v}=0 \end{array}\right. \quad \text{with} \quad \left|\begin{array}{l} f_0=\dfrac{F_0}{F^{+}} \\ \omega=\Omega\sqrt{\dfrac{M}{K_0}} \\ \zeta=\dfrac{C}{2\sqrt{MK_0}} \end{array}\right., \tag{8}$$

where ζ is the damping ratio. Correspondingly, the three states in the $(v,\dot{u})$ phase space are

$$\left|\begin{array}{l} \hat{E} \text{ state}: (-1-\varepsilon<v<1) \text{ or } [(v=1) \text{ and } (\dot{u}v\le 0)] \text{ or } [(v=-1-\varepsilon) \text{ and } (\dot{u}v\le 0)] \\ \hat{P}^{+} \text{ state}: (v=1) \text{ and } \dot{u}\ge 0. \\ \hat{P}^{-} \text{ state}: (v=-1-\varepsilon) \text{ and } \dot{u}\le 0. \end{array}\right. \tag{9}$$

III. EQUIVALENCE WITH THE ASYMMETRIC FORCING

Equivalence between asymmetric forcing and asymmetric strength is now investigated. Let us consider the symmetric elastic perfectly-plastic oscillator ($\varepsilon=0$) with an asymmetrical forcing term,

$$\left|\begin{array}{l} \hat{E} \text{ state: } M\ddot{U}+C\dot{U}+K_0(U-U_p)=F(t);\ \dot{U}_p=0 \\ \hat{P}^{+} \text{ state: } M\ddot{U}+C\dot{U}+F^{+}=F(t);\ \dot{U}_p=\dot{U} \\ \hat{P}^{-} \text{ state: } M\ddot{U}+C\dot{U}-F^{+}=F(t);\ \dot{U}_p=\dot{U} \end{array}\right. , \quad \text{with } F(t)=F_0\cos\Omega t+\Delta F_0. \tag{10}$$

Each state is defined from a partition of the phase space $(U,\dot{U},U_p)$.

$$\left|\begin{array}{l} \hat{E} \text{ state: } (|U-U_p|<U_Y) \text{ or } [(|U-U_p|=U_Y) \text{ and } (\dot{U}(U-U_p)\le 0)] \\ \hat{P}^{+} \text{ state: } (U-U_p=U_Y) \text{ and } \dot{U}\ge 0 \\ \hat{P}^{-} \text{ state: } (U-U_p=-U_Y) \text{ and } \dot{U}\le 0 \end{array}\right. . \tag{11}$$

The dimensionless variables (3)–(5), (7), and (8) are used,

$$\left|\begin{array}{l} \hat{E} \text{ state: } \ddot{u}+2\zeta\dot{u}+v=\Delta f_0+f_0\cos\omega\tau;\ \dot{v}=\dot{u} \\ \hat{P}^{+} \text{ state: } \ddot{u}+2\zeta\dot{u}+1=\Delta f_0+f_0\cos\omega\tau;\ \dot{v}=0 \\ \hat{P}^{-} \text{ state: } \ddot{u}+2\zeta\dot{u}-1=\Delta f_0+f_0\cos\omega\tau;\ \dot{v}=0 \end{array}\right. , \quad \text{with } \Delta f_0=\frac{\Delta F_0}{F^{+}}, \tag{12}$$

with the three states defined by

$$\left|\begin{array}{l} \hat{E} \text{ state: } (|v|<1) \text{ or } [(|v|=1) \text{ and } (\dot{u}v\le 0)] \\ \hat{P}^{+} \text{ state: } (v=1) \text{ and } \dot{u}\ge 0 \\ \hat{P}^{-} \text{ state: } (v=-1) \text{ and } \dot{u}\le 0 \end{array}\right. . \tag{13}$$

The following change of variables may be chosen:

$$\left|\begin{array}{l} \hat{u}=\dfrac{u}{1-\Delta f_0} \\ \hat{v}=\dfrac{v-\Delta f_0}{1-\Delta f_0} \end{array}\right. \quad \text{and} \quad \left|\begin{array}{l} \hat{f}_0=\dfrac{f_0}{1-\Delta f_0} \\ \hat{\varepsilon}=\dfrac{2\Delta f_0}{1-\Delta f_0} \end{array}\right. . \tag{14}$$

It is not difficult to convert Eq. (12) into

$$\begin{cases} \hat{E} \text{ state: } \ddot{\hat{u}} + 2\zeta\,\dot{\hat{u}} + \hat{v} = \hat{f}_0 \cos\omega\tau;\ \dot{\hat{v}} = \dot{\hat{u}} \\ \hat{P}^+ \text{ state: } \ddot{\hat{u}} + 2\zeta\dot{\hat{u}} + 1 = \hat{f}_0 \cos\omega\tau;\ \dot{\hat{v}} = 0 \\ \hat{P}^- \text{ state: } \ddot{\hat{u}} + 2\zeta\dot{\hat{u}} - (1+\hat{\varepsilon}) = \hat{f}_0 \cos\omega\tau;\ \dot{\hat{v}} = 0 \end{cases}, \tag{15}$$

with the following definition of each state:

$$\begin{cases} \hat{E} \text{ state: } (-1-\hat{\varepsilon} < \hat{v} < 1) \text{ or } [(\hat{v} = 1) \text{ and } (\dot{\hat{u}}\hat{v} \le 0)] \text{ or } [(\hat{v} = -1-\hat{\varepsilon}) \text{ and } (\dot{\hat{u}}\hat{v} \le 0)] \\ \hat{P}^+ \text{ state: } (\hat{v} = 1) \text{ and } \dot{\hat{u}} \ge 0 \\ \hat{P}^- \text{ state: } (\hat{v} = -1-\hat{\varepsilon}) \text{ and } \dot{\hat{u}} \le 0 \end{cases}. \tag{16}$$

One recognizes in Eqs. (15) and (16) the system of Eqs. (8) and (9) with the new variables. In other words, considering a strength asymmetry ($|F^-| \neq |F^+|$) or a forcing asymmetry ($\Delta F_0 \neq 0$) is strictly equivalent for this simple structural system. For the following, the initial dynamic system Eqs. (8) and (9) will be studied.

IV. FORCED VIBRATIONS: ANALYSIS

A. Governing equations

As for general piecewise linear oscillators, solutions of the periodically forced oscillator Eq. (8) are known explicitly for each state. The initial conditions at the beginning of each state are written by

$$[v(\tau_i), \dot{u}(\tau_i)] = (v_i, \dot{u}_i). \tag{17}$$

The solution to the $\hat{E}$ state can be calculated as

$$\begin{aligned} v(\tau) = &\left[\left(\cos(\sqrt{1-\zeta^2}(\tau-\tau_i)) \left(v_i - f_0 \frac{(1-\omega^2)\cos(\omega\tau_i) + 2\omega\zeta\sin(\omega\tau_i)}{(1-\omega^2)^2 + 4\omega^2\zeta^2} \right) \right.\right. \\ &\left.\left. + \sin(\sqrt{1-\zeta^2}(\tau-\tau_i)) \left(\frac{v_i\zeta + \dot{u}_i}{\sqrt{1-\zeta^2}} + f_0 \frac{-\zeta(1+\omega^2)\cos(\omega\tau_i) + \omega(1-\omega^2-2\zeta^2)\sin(\omega\tau_i)}{\sqrt{1-\zeta^2}((1-\omega^2)^2 + 4\omega^2\zeta^2)} \right) \right] \right. \\ &\left. \times e^{-\zeta(\tau-\tau_i)} + f_0 \frac{(1-\omega^2)\cos(\omega\tau) + 2\omega\zeta\sin(\omega\tau)}{(1-\omega^2)^2 + 4\zeta^2\omega^2} \right. \end{aligned} \tag{18}$$

$$\begin{aligned} \dot{u}(\tau) = &\left\{ \left(\cos[\sqrt{1-\zeta^2}(\tau-\tau_i)) \left(\dot{u}_i + f_0 \left(\frac{-2\omega^2\zeta\cos(\omega\tau_i) + \omega(1-\omega^2)\sin(\omega\tau_i)}{(1-\omega^2)^2 + 4\omega^2\zeta^2} \right) \right) \right.\right. \\ &\left.\left. + \sin(\sqrt{1-\zeta^2}(\tau-\tau_i)) \left(-\frac{v_i + \dot{u}_i\zeta}{\sqrt{1-\zeta^2}} + f_0 \frac{\cos(\omega\tau_i)(2\omega^2\zeta^2 + 1 - \omega^2) + \sin(\omega\tau_i)(\omega\zeta(1+\omega^2))}{\sqrt{1-\zeta^2}((1-\omega^2)^2 + 4\omega^2\zeta^2)} \right) \right\} \right. \\ &\left. \times e^{-\zeta(\tau-\tau_i)} + \omega f_0 \frac{2\omega\zeta\cos(\omega\tau) - (1-\omega^2)\sin(\omega\tau)}{(1-\omega^2)^2 + 4\zeta^2\omega^2} \right. \end{aligned}$$

The solution to the $\hat{P}$ state can be calculated as

$$\begin{cases} v(\tau) = v_i = 1 \text{ or } v(\tau) = v_i = -1-\varepsilon \\ \dot{u}(\tau) = \left(\dot{u}_i + \dfrac{v_i}{2\zeta} - f_0 \dfrac{2\zeta\cos(\omega\tau_i) + \omega\sin(\omega\tau_i)}{4\zeta^2 + \omega^2} \right) e^{-2\zeta(\tau-\tau_i)} - \dfrac{v_i}{2\zeta} + f_0 \dfrac{2\zeta\cos(\omega\tau) + \omega\sin(\omega\tau)}{4\zeta^2 + \omega^2} \end{cases} \tag{19}$$

Piecing together these known solutions is not directly possible, however, since the time of flight in each region (each state) cannot be found in closed-form solution for the forced oscillator. The method of locating events is used in the integration process (see, for instance, [42]). For the initial conditions specified, the computer solves the crossing time τ_{i+1} using a simple Newton–Raphson method. The nonlinear equation to be solved is given by Eq. (18) when the initial state is elastic:

$$v(\tau_{i+1}) = 1 \quad \text{or } v(\tau_{i+1}) = -1-\varepsilon, \tag{20}$$

whereas the nonlinear equation to be solved is given by Eq. (19) when the initial state is plastic,

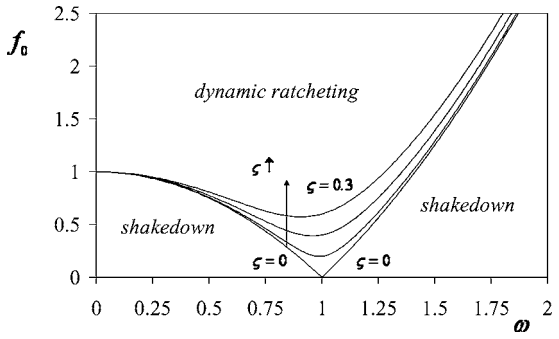

FIG. 5. Boundary between elastoplastic shakedown and dynamic ratcheting in the space (ω, f_0); $\zeta \in \{0, 0.1, 0.2, 0.3\}$; $\varepsilon > 0$.

$$\dot{u}(\tau_{i+1}) = 0. \tag{21}$$

The new time τ_{i+1} is used for the equation of motion in the new region encountered. This method is considerably more accurate than usual numerical solutions of ordinary differential equations, the only approximation being made on the calculation of the crossing time.

B. Numerical analysis

The numerical analysis is performed for strictly positive damping ratios ($\zeta > 0$). All trajectories tend toward periodic orbits, which can be viewed as "limit cycles" in the $(v, \dot{u})$ space. These "limit cycles" do not depend on initial conditions. In reality, the periodic orbits are completely characterized in the $(v, \dot{u}, \tau)$ space. Numerical simulations show that these periodic orbits are asymptotically stable for all perturbations. In this sense, the behavior of the damped elastoplastic oscillator is much simpler than the one of the undamped one, which does not possess this fundamental property (see [41]). The period of these limit cycles is equal to $2\pi/\omega$. The shape of these limit cycles depends on the values of the structural parameters $(f_0, \omega, \zeta, \varepsilon)$. Shakedown (elastic stationary evolutions) is described by a smooth limit cycle, whereas alternating plasticity is depicted by nonsmooth cycles. It means that these two basic phenomena can be differentiated by simple geometrical arguments in the phase space. Moreover, in the asymmetric case $(\varepsilon \neq 0)$, all the limit cycles involving plastic phases are asymmetrical cycles (no central symmetry with respect to the origin point). As a consequence of this lack of symmetry, the periodic nature in the reduced space $(v, \dot{u})$ leads to the divergence in the initial space $(u, u_p, \dot{u})$. Ratcheting is then observed in the asymmetric case $(\varepsilon \neq 0)$, whereas alternating plasticity with bounded evolutions is observed in the symmetric case $(\varepsilon = 0)$ (see Figs. 3 and 4). As a consequence, the shakedown boundary is also a dynamic ratcheting boundary for the asymmetric case.

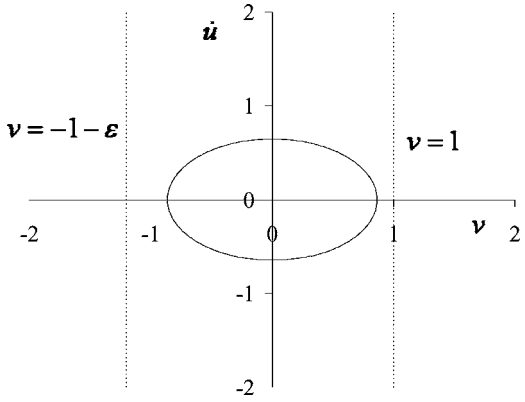

FIG. 6. Elastoplastic shakedown: $\zeta=0.1$; $f_0=0.4$; $\omega=0.75$; $\varepsilon=0.2$.

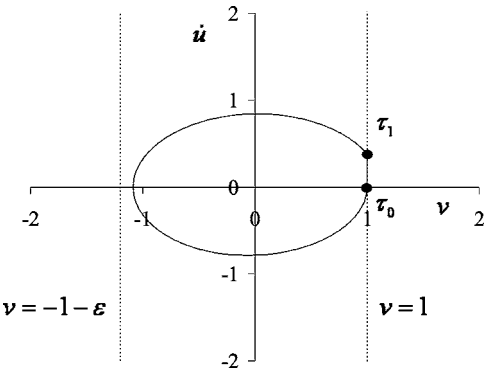

FIG. 7. Determination of the characteristic times for the (1,1) periodic orbit: $\zeta=0.1$; $f_0=0.5$; $\omega=0.75$; $\varepsilon=0.2$.

The equation of the limit cycle in the shakedown area is obtained from Eq. (18) by considering only the stationary term,

$$\begin{vmatrix} v(\tau) = f_0 \dfrac{(1-\omega^2)\cos(\omega\tau) + 2\omega\zeta \sin(\omega\tau)}{(1-\omega^2)^2 + 4\zeta^2\omega^2} \\ \dot{u}(\tau) = \omega f_0 \dfrac{2\omega\zeta \cos(\omega\tau) - (1-\omega^2)\sin(\omega\tau)}{(1-\omega^2)^2 + 4\zeta^2\omega^2} \end{vmatrix}. \tag{22}$$

This is a centered ellipse whose equation is given by

$$\frac{v^2}{a^2} + \frac{\dot{u}^2}{b^2} = 1, \quad \text{with } a = \frac{f_0}{\sqrt{(1-\omega^2)^2 + 4\omega^2\zeta^2}} \text{ and } b = a\omega. \tag{23}$$

The equation of the limit cycle at the boundary between shakedown and alternating plasticity is obtained when the

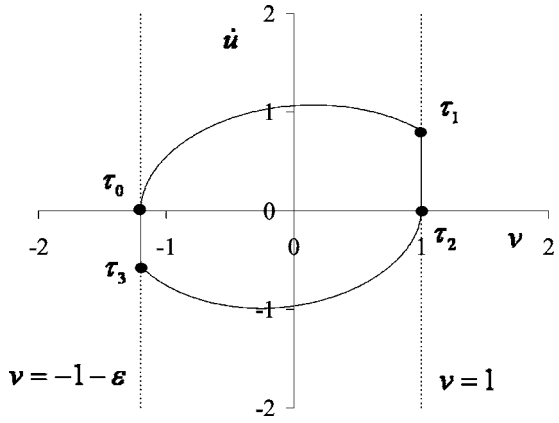

FIG. 8. Determination of the characteristic times for the (1, 2) periodic orbit: $\zeta=0.1$; $f_0=0.6$; $\omega=0.75$; $\varepsilon=0.2$.

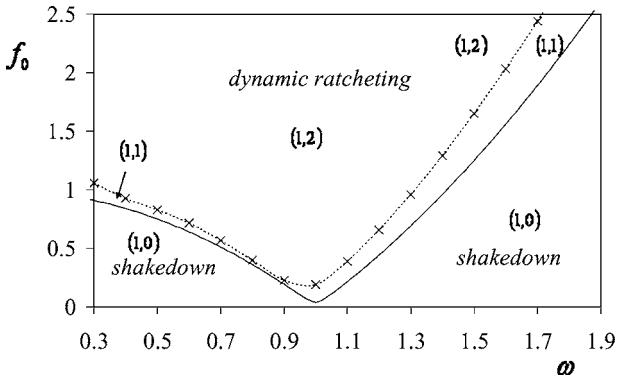

FIG. 9. Boundary between the (1,0), (1,1), and the (1,2) periodic orbit: ζ=0.02; ε=0.2.

ellipse parameter a is equal to 1 in Eq. (23), i.e.,

$$f_0 = \sqrt{(1-\omega^2)^2 + 4\omega^2\zeta^2}. \tag{24}$$

In this case, the equation of the ellipse which is tangent to the axis $v=1$ is reduced to

$$v^2 + \frac{\dot{u}^2}{\omega^2} = 1. \tag{25}$$

This boundary between shakedown and alternating plasticity was already investigated by Liu and Huang [30] or Challamel [31] for the symmetrical oscillator. In case of the undamped system, Eq. (24) can be simplified by

$$f_0 = |1-\omega^2|. \tag{26}$$

The boundary (24) is graphically represented in Fig. 5. The periodic alternating plasticity motion can be classified, as for instance by Awrejcewicz and Lamarque [14], for mechanical systems with impacts. We will call (n,k) periodic solution of period nT with k plastic phases per cycle, where $T=(2\pi/\omega)$ is the period of the external excitation. Within this classification, most of the simulations exhibit stable (1,1) or (1,2) periodic solutions. The shakedown orbit is represented in Fig. 6, whereas the (1,1) and (1,2) periodic orbits are shown in Figs. 7 and 8. The boundary between the (1,1) and the (1,2) periodic region is represented in Fig. 9 (ζ=0.02; ε=0.2). With the parameters of interest, only (1,0), (1,1), and (1,2) periodic orbits have been observed for ω greater than 0.3. However, $(1,n)$ periodic orbits have been captured for smaller angular frequencies, with n greater than 2. For instance, (1,3) periodic orbit is shown in Fig. 10, (1,4) periodic orbit in Fig. 11, (1,5) periodic orbit in Fig. 12, and (1,6) periodic orbit in Fig. 13. The bifurcation diagram of Fig. 14 highlights the transition between each type of periodic orbit. It can be noticed that the fundamental difference with the bifurcation diagram of the symmetrical case (ε=0) is that the number of plastic phases can be even or odd when $\varepsilon \neq 0$. The following part is focused on the characterization of the most common periodic solutions, the (1,1) and the (1,2) periodic orbits, according to their stability properties.

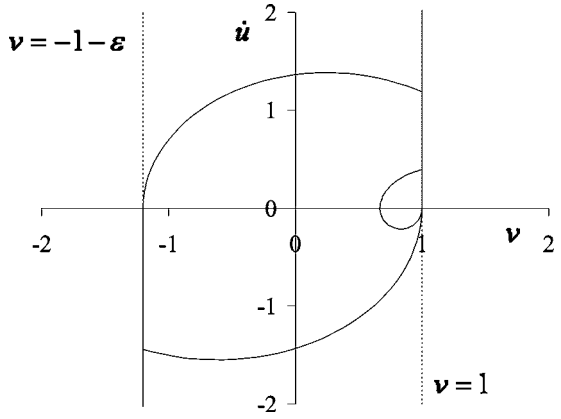

FIG. 10. (1,3) periodic orbit: ω=0.065; ζ=0.02; f_0=2; ε=0.2.

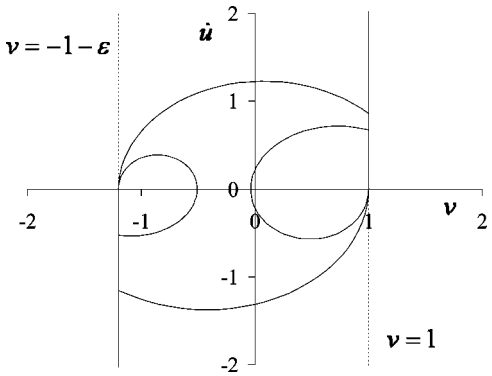

FIG. 11. (1,4) periodic orbit: ω=0.05; ζ=0.02; f_0=2; ε=0.2.

V. FORCED VIBRATIONS: CLOSED-FORM SOLUTION OF THE (1,1) PERIODIC ORBIT

The existence and uniqueness of a periodic (1,1) solution is treated in this part. The methodology is based on the fact that the duration in each phase (one elastic phase and one plastic phase) is exactly equal to the period of the cycle,

$$\tau_2(\tau_0) - \tau_0 = \frac{2\pi}{\omega}, \tag{27}$$

where τ_0 is the time at the beginning of the elastic phase following the plastic phase $\hat{P}^+$, τ_1 is the time at the end of

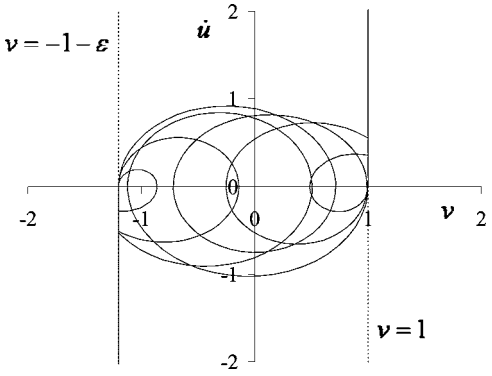

FIG. 12. (1,5) periodic orbit: ω=0.03; ζ=0.02; f_0=2; ε=0.2.

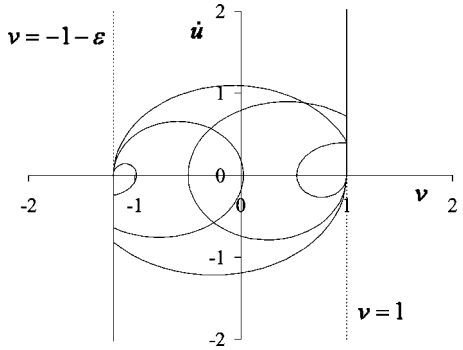

FIG. 13. (1,6) periodic orbit: ω=0.04; ζ=0.02; f_0=2; ε=0.2.

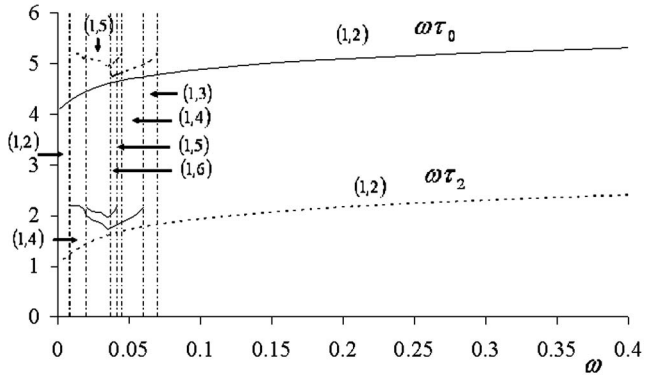

FIG. 14. Bifurcation diagram: ζ=0.02; f_0=2; ε=0.2.

this elastic phase, and τ_2 is the time at the end of the plastic phase $\hat{P}^+$ (see Fig. 7). The most general method needs the resolution of the following nonlinear system of three functions, defined by Eqs. (18) and (19):

$$\left|\begin{array}{l} \hat{E} \text{ state: } v(\tau_0,\tau_1)=1;\ \dot{u}_1=\dot{u}(\tau_0,\tau_1) \\ \hat{P}^+ \text{ state: } \dot{u}(\tau_1,\tau_2,\dot{u}_1)=0 \\ \tau_2-\tau_0=\dfrac{2\pi}{\omega} \end{array}\right. . \tag{28}$$

This system can simply be reduced to two nonlinear functions,

$$\left|\begin{array}{l} \hat{E} \text{ state: } v(\tau_0,\tau_1)=1;\ \dot{u}_1=\dot{u}(\tau_0,\tau_1) \\ \hat{P}^+ \text{ state: } \dot{u}\left(\tau_1,\tau_0+\dfrac{2\pi}{\omega},\dot{u}_1\right)=0 \end{array}\right. , \tag{29}$$

which can be expressed by

$$\left[\cos(\sqrt{1-\zeta^2}(\tau_1-\tau_0))\left(1-f_0\frac{(1-\omega^2)\cos(\omega\tau_0)+2\omega\zeta\sin(\omega\tau_0)}{(1-\omega^2)^2+4\omega^2\zeta^2}\right)\right.$$
$$\left.+\sin[\sqrt{1-\zeta^2}(\tau_1-\tau_0))\left(\frac{\zeta}{\sqrt{1-\zeta^2}}+f_0\frac{-\zeta(1+\omega^2)\cos(\omega\tau_0)+\omega(1-\omega^2-2\zeta^2)\sin(\omega\tau_0)}{\sqrt{1-\zeta^2}((1-\omega^2)^2+4\omega^2\zeta^2)}\right)\right]e^{-\zeta(\tau_1-\tau_0)}$$
$$+f_0\frac{(1-\omega^2)\cos(\omega\tau_1)+2\omega\zeta\sin(\omega\tau_1)}{(1-\omega^2)^2+4\zeta^2\omega^2}=1$$

$$\left(\dot{u}_1(\tau_0,\tau_1)+\frac{1}{2\zeta}-f_0\frac{2\zeta\cos(\omega\tau_1)+\omega\sin(\omega\tau_1)}{4\zeta^2+\omega^2}\right)e^{-2\zeta\left(\tau_0+\frac{2\zeta}{\omega}-\tau_1\right)}-\frac{1}{2\zeta}+f_0\frac{2\zeta\cos(\omega\tau_0)+\omega\sin(\omega\tau_0)}{4\zeta^2+\omega^2}=0$$

with

$$\dot{u}_1=\left\{\left(\cos[\sqrt{1-\zeta^2}(\tau_1-\tau_0)]f_0\left(\frac{-2\omega^2\zeta\cos(\omega\tau_0)+\omega(1-\omega^2)\sin(\omega\tau_0)}{(1-\omega^2)^2+4\omega^2\zeta^2}\right)\right.\right.$$
$$\left.\left.+\sin[\sqrt{1-\zeta^2}(\tau_1-\tau_0)]\left(\frac{-1}{\sqrt{1-\zeta^2}}+f_0\frac{\cos(\omega\tau_0)(2\omega^2\zeta^2+1-\omega^2)+\sin(\omega\tau_0)[\omega\zeta(1+\omega^2)]}{\sqrt{1-\zeta^2}[(1-\omega^2)^2+4\omega^2\zeta^2]}\right)\right\}\right.$$
$$\times e^{-\zeta(\tau_1-\tau_0)}+\omega f_0\frac{2\omega\zeta\cos(\omega\tau_1)-(1-\omega^2)\sin(\omega\tau_1)}{(1-\omega^2)^2+4\zeta^2\omega^2}, \tag{30}$$

It is possible to write the complex system Eq. (29) as

$$\begin{vmatrix} \hat{A}\cos(\omega\tau_0)+\hat{B}\sin(\omega\tau_0)=\hat{C} \\ \hat{D}\cos(\omega\tau_0)+\hat{E}\sin(\omega\tau_0)=\hat{F} \end{vmatrix}, \tag{31}$$

where the coefficients $\hat{A}$, $\hat{B}$, $\hat{C}$, $\hat{D}$, $\hat{E}$, and $\hat{F}$ depend on the structural parameters (ω,ζ,f_0) but also on the time variable $\bar{y}=\tau_1-\tau_0$ (see Appendix A). As remarked by Liu and Huang [30] for the symmetrical oscillator, this system can be merged into one single nonlinear equation of $\bar{y}$,

$$(\hat{C}\hat{D}-\hat{A}\hat{F})^2+(\hat{C}\hat{E}-\hat{B}\hat{F})^2=(\hat{A}\hat{E}-\hat{B}\hat{D})^2. \tag{32}$$

The time τ_0 follows from the computation of the trigonometrical equation

$$\begin{vmatrix} \cos(\omega\tau_0)=\dfrac{\hat{C}\hat{E}-\hat{B}\hat{F}}{\hat{A}\hat{E}-\hat{B}\hat{D}} \\ \sin(\omega\tau_0)=\dfrac{-\hat{C}\hat{D}+\hat{A}\hat{F}}{\hat{A}\hat{E}-\hat{B}\hat{D}} \end{vmatrix} \quad \text{if } \hat{A}\hat{E}-\hat{B}\hat{D}\neq 0. \tag{33}$$

For the (1,1) solution, one also has to verify some inequalities (see the discussion in [31]),

$$\hat{E} \text{ state: } \forall\ \tau\in[\tau_0,\tau_1], -1-\varepsilon<v(\tau)<-1$$

and

$$\hat{P}^+ \text{ state: } \forall\ \tau\in[\tau_1,\tau_2], \dot{u}(\tau)\geq 0. \tag{34}$$

VI. STABILITY ANALYSIS OF THE (1,1) PERIODIC ORBIT

The stability analysis of the $(1,1)$ periodic orbit is based on a perturbation technique introduced by Masri and Caughey [24].

$$\begin{pmatrix} \Delta\tau_0 \\ \Delta v_0 \\ \Delta\dot{u}_0 \end{pmatrix} \rightarrow \begin{pmatrix} \Delta\tau_1 \\ \Delta v_1 \\ \Delta\dot{u}_1 \end{pmatrix} \rightarrow \begin{pmatrix} \Delta\tau_2 \\ \Delta v_2 \\ \Delta\dot{u}_2 \end{pmatrix}$$

with

$$\Delta v_0=\Delta\dot{u}_0=\Delta v_1=\Delta v_2=\Delta\dot{u}_2=0. \tag{35}$$

The following matrices **A** and **B** can be introduced for the propagation of errors:

$$\begin{pmatrix} \Delta\tau_1 \\ \Delta v_1 \\ \Delta\dot{u}_1 \end{pmatrix} = \begin{pmatrix} A_{11} & A_{12} & A_{13} \\ A_{21} & A_{22} & A_{23} \\ A_{31} & A_{32} & A_{33} \end{pmatrix} \begin{pmatrix} \Delta\tau_0 \\ \Delta v_0 \\ \Delta\dot{u}_0 \end{pmatrix}$$

and

$$\begin{pmatrix} \Delta\tau_2 \\ \Delta v_2 \\ \Delta\dot{u}_2 \end{pmatrix} = \begin{pmatrix} B_{11} & B_{12} & B_{13} \\ B_{21} & B_{22} & B_{23} \\ B_{31} & B_{32} & B_{33} \end{pmatrix} \begin{pmatrix} \Delta\tau_1 \\ \Delta v_1 \\ \Delta\dot{u}_1 \end{pmatrix}. \tag{36}$$

Equations (35) and (36) lead to the scalar equation

$$\Delta\tau_2=R\Delta\tau_0 \quad \text{with } R=A_{11}B_{11}+A_{31}B_{13}. \tag{37}$$

The value of R determines the stability of the solution [24]. The $(1,1)$ solution is asymptotically stable if the modulus of R is less than unity. If the modulus of R is greater than one, the solution is unstable. A bifurcation may occur when the modulus takes the value of unity. The coefficients that appear in the calculation of R are given in Appendix B. R can be finally simplified in

$$R=e^{-\zeta\left(\tau_0-\tau_1+\frac{4\pi}{\omega}\right)}\left\{\cos[\sqrt{1-\zeta^2}(\tau_1-\tau_0)] - \frac{\zeta}{\sqrt{1-\zeta^2}}\sin[\sqrt{1-\zeta^2}(\tau_1-\tau_0)]\right\}. \tag{38}$$

In the case of the undamped system, this coefficient is reduced to

$$|R(\zeta=0)|=|\cos(\tau_1-\tau_0)|\leq 1. \tag{39}$$

Generally, $|R|$ is strictly less than unity ($\tau_1\neq\tau_0+n\pi$). This means that the $(1,1)$ periodic orbit (when it exists) is always asymptotically stable for the undamped system. It can be numerically checked that Eq. (38) leads to the same conclusion for the damped system.

VII. STABILITY ANALYSIS OF THE (1, 2) PERIODIC ORBIT

This (1,2) periodic orbit is characterized by four crossing times (see Fig. 8). τ_0 is the time at the beginning of the elastic phase following the plastic phase $\hat{P}^-$, τ_1 is the time at the end of this elastic phase, τ_2 is the time at the end of the plastic phase $\hat{P}^+$, τ_3 is the time at the beginning of the plastic phase $\hat{P}^+$, and τ_4 is the time at the end of this plastic phase. As the motion is periodic, one has

$$\tau_4(\tau_0)-\tau_0=\frac{2\pi}{\omega}. \tag{40}$$

The most general method needs the resolution of a nonlinear system of five functions, defined by Eqs. (18) and (19):

$$\begin{vmatrix} \hat{E} \text{ state: } v(\tau_0,\tau_1)=1;\ \dot{u}_1=\dot{u}(\tau_0,\tau_1) \\ \hat{P}^+ \text{ state: } \dot{u}(\tau_1,\tau_2,\dot{u}_1)=0 \\ \hat{E} \text{ state: } v(\tau_2,\tau_3)=1;\ \dot{u}_3=\dot{u}(\tau_2,\tau_3) \\ \hat{P}^- \text{ state: } \dot{u}(\tau_3,\tau_4,\dot{u}_3)=0 \\ \tau_4-\tau_0=\dfrac{2\pi}{\omega} \end{vmatrix}. \tag{41}$$

Once this system is numerically solved, the stability analysis of the $(1,2)$ periodic orbit is similar to the one developed for the $(1,1)$ periodic orbit. The amplification factor $R_i; i\in\{1,2\}$ may be introduced from

$$\Delta\tau_2=R'\Delta\tau_0 \quad \text{and} \quad \Delta\tau_4=R''\Delta\tau_2. \tag{42}$$

The stability analysis depends on the value of R,

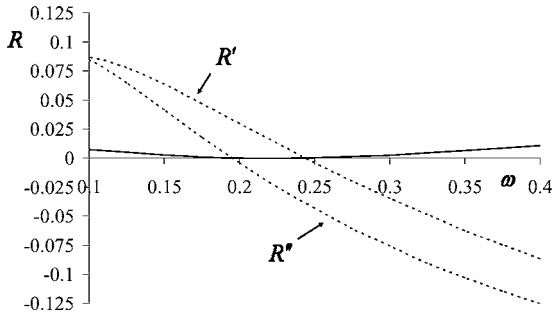

FIG. 15. Stability of the (1, 2) periodic orbit: $\zeta=0.02$; $f_0=2$; $\varepsilon=0.2$.

$$\Delta\tau_4 = R\Delta\tau_0 \quad \text{with } R = R'R''. \tag{43}$$

The calculation of R is detailed in Appendix C and leads to

$$R = e^{-2\zeta(\tau_4-\tau_3+\tau_2-\tau_1)}e^{-\zeta(\tau_3-\tau_2+\tau_1-\tau_0)}\left\{-\cos[\sqrt{1-\zeta^2}(\tau_3-\tau_2)] + \frac{\zeta}{\sqrt{1-\zeta^2}}\sin[\sqrt{1-\zeta^2}(\tau_3-\tau_2)]\right\}\left\{-\cos[\sqrt{1-\zeta^2}(\tau_1-\tau_0)] + \frac{\zeta}{\sqrt{1-\zeta^2}}\sin[\sqrt{1-\zeta^2}(\tau_1-\tau_0)]\right\}. \tag{44}$$

In the case of the undamped system ($\zeta=0$), the amplification factor is reduced to

$$R = \{\cos(\tau_3-\tau_2)\}\{\cos(\tau_1-\tau_0)\}. \tag{45}$$

Equation (45) clearly indicates that the modulus of R is less than unity. This new result means that the asymmetrical (1,2) periodic orbit is asymptotically stable for the undamped system. It can be numerically checked that Eq. (45) leads to the same conclusion for the damped system. The variation of R with respect to ω is given in Fig. 15, which confirms the asymptotic stability property.

VIII. RATCHETING: RATE OF DIVERGENCE

When ratcheting prevails, it is interesting to quantify the divergence rate to characterize the route to collapse. Let us introduce the divergence factor $\bar{\dot{u}}$ (mean value of the rate of displacement)

$$\bar{\dot{u}} = \frac{1}{T}\int_{\tau_0}^{\tau_0+T} \dot{u}(\tau)d\tau. \tag{46}$$

In the case of (1,2) periodic orbits, the divergence factor can be written as

$$\bar{\dot{u}} = \frac{\omega}{2\pi}[u(\tau_4)-u(\tau_0)]. \tag{47}$$

The integral calculation may be decomposed into the following four parts:

$$\bar{\dot{u}} = \frac{\omega}{2\pi}\left[\int_{\tau_0}^{\tau_1}\dot{u}(\tau)d\tau + \int_{\tau_1}^{\tau_2}\dot{u}(\tau)d\tau + \int_{\tau_2}^{\tau_3}\dot{u}(\tau)d\tau + \int_{\tau_3}^{\tau_4}\dot{u}(\tau)d\tau\right]. \tag{48}$$

In the elastic phases, the integral may be easily simplified by

$$\int_{\tau_0}^{\tau_1}\dot{u}(\tau)d\tau = \int_{\tau_0}^{\tau_1}\dot{v}(\tau)d\tau = v(\tau_1)-v(\tau_0) = 2+\varepsilon \tag{49}$$

and

$$\int_{\tau_2}^{\tau_3}\dot{u}(\tau)d\tau = v(\tau_3)-v(\tau_2) = -(2+\varepsilon).$$

Finally, the determination of the divergence rate $\bar{\dot{u}}$ needs only the calculation of the two integral terms

$$\bar{\dot{u}} = \frac{\omega}{2\pi}\left[\int_{\tau_1}^{\tau_2}\dot{u}(\tau)d\tau + \int_{\tau_3}^{\tau_4}\dot{u}(\tau)d\tau\right], \tag{50}$$

where only the plastic phases control the evolution of $\dot{u}$, given by Eq. (19). The calculation leads to the following result:

$$\begin{aligned}\bar{\dot{u}} = &-\frac{\omega}{4\pi\zeta}(e^{-2\zeta(\tau_2-\tau_1)}-1)\left(\dot{u}_1+\frac{1}{2\zeta} - f_0\frac{2\zeta\cos(\omega\tau_1)+\omega\sin(\omega\tau_1)}{4\zeta^2+\omega^2}\right) - \frac{\omega}{4\pi\zeta}(\tau_2-\tau_1)\\ &+\frac{f_0}{4\zeta^2+\omega^2}\left\{\frac{\zeta}{\pi}[\sin(\omega\tau_2)-\sin(\omega\tau_1)] - \frac{\omega}{2\pi}[\cos(\omega\tau_2) - \cos(\omega\tau_1)]\right\} - \frac{\omega}{4\pi\zeta}(e^{-2\zeta(\tau_4-\tau_3)}-1)\left(\dot{u}_3-\frac{1+\varepsilon}{2\zeta}\right.\\ &\left.-f_0\frac{2\zeta\cos(\omega\tau_3)+\omega\sin(\omega\tau_3)}{4\zeta^2+\omega^2}\right) + (1+\varepsilon)\frac{\omega}{4\pi\zeta}(\tau_4-\tau_3)\\ &+\frac{f_0}{4\zeta^2+\omega^2}\left\{\frac{\zeta}{\pi}[\sin(\omega\tau_4)-\sin(\omega\tau_3)] - \frac{\omega}{2\pi}[\cos(\omega\tau_4) - \cos(\omega\tau_3)]\right\}.\end{aligned} \tag{51}$$

Equation (51) can be directly expressed in terms of the time characteristics $(\tau_1,\tau_2,\tau_3,\tau_4)$.

$$\begin{aligned}\bar{\dot{u}} = &-\frac{\omega}{4\pi\zeta}(1-e^{2\zeta(\tau_2-\tau_1)})\left(\frac{1}{2\zeta} - f_0\frac{2\zeta\cos(\omega\tau_2)+\omega\sin(\omega\tau_2)}{4\zeta^2+\omega^2}\right)\\ &-\frac{\omega}{4\pi\zeta}(\tau_2-\tau_1) + \frac{f_0}{4\zeta^2+\omega^2}\left\{\frac{\zeta}{\pi}[\sin(\omega\tau_2)-\sin(\omega\tau_1)]\right.\\ &\left.-\frac{\omega}{2\pi}[\cos(\omega\tau_2)-\cos(\omega\tau_1)]\right\} - \frac{\omega}{4\pi\zeta}(1-e^{2\zeta(\tau_4-\tau_3)})\\ &\times\left(-\frac{1+\varepsilon}{2\zeta} - f_0\frac{2\zeta\cos(\omega\tau_4)+\omega\sin(\omega\tau_4)}{4\zeta^2+\omega^2}\right) + (1\end{aligned}$$

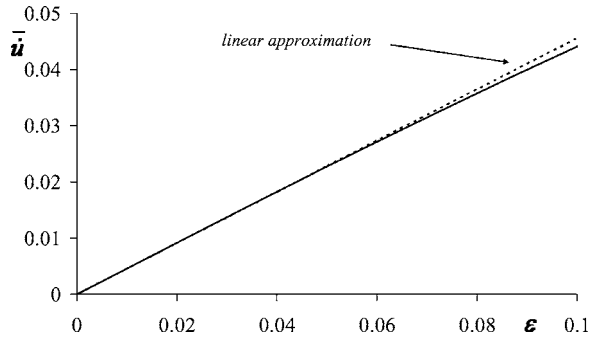

FIG. 16. Evolution of the divergence factor $\bar{\dot{u}}$ versus the asymmetrical parameter ε: $\zeta=0.1$; $f_0=0.8$; $\omega=0.75$.

$$+\varepsilon)\frac{\omega}{4\pi\zeta}(\tau_4-\tau_3)+\frac{f_0}{4\zeta^2+\omega^2}\left\{\frac{\zeta}{\pi}[\sin(\omega\tau_4)-\sin(\omega\tau_3)]\right.$$
$$\left.-\frac{\omega}{2\pi}[\cos(\omega\tau_4)-\cos(\omega\tau_3)]\right\} \tag{52}$$

It is easy to verify from Eq. (52) that no ratcheting prevails for the symmetrical system with positive damping values [31].

$$\varepsilon=0\Rightarrow\left|\begin{array}{l}\tau_4=\tau_2+\dfrac{\pi}{\omega}\\ \tau_3=\tau_1+\dfrac{\pi}{\omega}\end{array}\right.\Rightarrow\bar{\dot{u}}=0. \tag{53}$$

The divergence factor $\bar{\dot{u}}$ is computed from Eq. (52) as a function of the asymmetric parameter ε (see Fig. 16). Figure 16 shows that the displacement rate $\bar{\dot{u}}$ increases as ε increases, and the proportionality rule may constitute a good approximation for sufficiently small values of ε,

$$\bar{\dot{u}}\propto\varepsilon. \tag{54}$$

Moreover, a threshold effect of ratcheting phenomenon is highlighted for sufficiently large values of ε, where the rate of divergence does not depend anymore on the asymmetric parameter ε (see Fig. 17). This threshold effect is linked to the transition between the $(1,2)$ periodic orbit to the $(1,1)$ periodic orbit. In case of $(1,1)$ periodic orbit, the divergence factor $\bar{\dot{u}}$ is calculated from

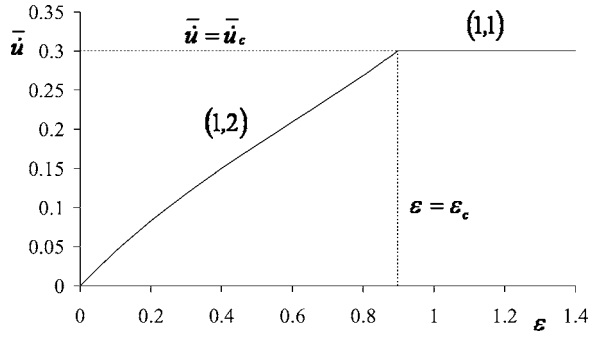

FIG. 17. Evolution of the divergence factor $\bar{\dot{u}}$ versus the asymmetrical parameter ε. Threshold effect for the ratcheting phenomenon: $\zeta=0.1$; $f_0=0.8$; $\omega=0.75$.

$$\bar{\dot{u}}=-\frac{\omega}{4\pi\zeta}(1-e^{2\zeta(\tau_2-\tau_1)})\left(\frac{1}{2\zeta}-f_0\frac{2\zeta\cos(\omega\tau_2)+\omega\sin(\omega\tau_2)}{4\zeta^2+\omega^2}\right)$$
$$-\frac{\omega}{4\pi\zeta}(\tau_2-\tau_1)+\frac{f_0}{4\zeta^2+\omega^2}\left\{\frac{\zeta}{\pi}[\sin(\omega\tau_2)-\sin(\omega\tau_1)]\right.$$
$$\left.-\frac{\omega}{2\pi}[\cos(\omega\tau_2)-\cos(\omega\tau_1)]\right\}. \tag{55}$$

In this case (for sufficiently large values of ε), the divergence factor does not depend on ε. From a general point of view, when the ratcheting threshold is not reached, ratcheting divergence is more pronounced for a highly asymmetrical oscillator. This result can be analyzed in the light of other mechanical studies devoted to ratcheting phenomenon, linked to an asymmetrical forcing term. Asymmetrical forcing may be mainly subdivided into two categories: the asymmetrical forcing term may provide from a drift, like in Pavlovskaia *et al.* [11] or in the present study ($\Delta f_0\neq 0$); the asymmetrical forcing term may also provide from a periodical asymmetrical forcing term, as in Ahn *et al.* [12]. It can be interesting to investigate this last case, constituted of a symmetric elastoplastic oscillator subjected to a dual-frequency sinusoidal excitation. The forcing term may be written as (which is more restrictive than the general cases treated in [12])

$$f(\tau)=f_0\cos\omega\tau+f_1\cos n\omega\tau,\quad\text{with } n \text{ integer}. \tag{56}$$

It is easy to verify that

$$\bar{f}=\frac{1}{T}\int_0^T f(\tau)d\tau=0. \tag{57}$$

f is periodical with period $T=2\pi/\omega$. However, the following symmetry property is not systematically verified (see [9]):

$$f\left(\tau+\frac{T}{2}\right)=-f(\tau). \tag{58}$$

The result follows:

$$\left|\begin{array}{l}n=2p\Rightarrow f\left(\tau+\dfrac{T}{2}\right)\neq-f(\tau)\\ n=2p+1\Rightarrow f\left(\tau+\dfrac{T}{2}\right)=-f(\tau)\end{array}\right.,\quad\text{with } p \text{ integer}. \tag{59}$$

The simple result is finally obtained outside the shakedown area

$$\left|\begin{array}{l}n=2p\Rightarrow\text{ratchet}\\ n=2p+1\Rightarrow\text{no ratchet}\end{array}\right.. \tag{60}$$

These results are confirmed by the simulations of Ahn *et al.* [12]. The case of n odd prevents the ratcheting phenomenon. On the opposite, dynamic ratcheting may develop when the ratio of applied frequency is an even number.

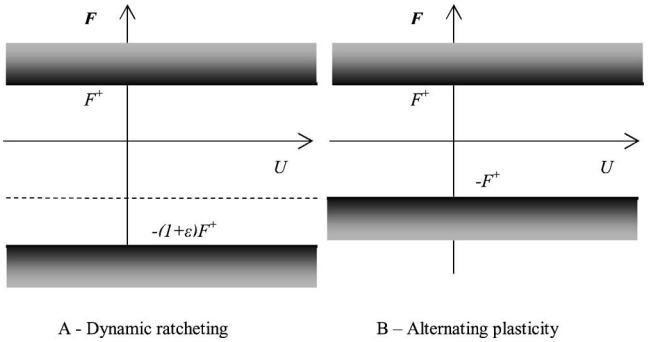

FIG. 18. Comparison of two strength domains, leading to bounded (case B) or unbounded evolutions (case A), outside the shakedown area.

Finally, a simple conclusion may be illustrated by the comparison of Fig. 18. The symmetric configuration is stabilizing (symmetry of loading, or symmetry of strength domain). On the contrary, asymmetrical configuration generally leads to dynamic ratcheting, or incremental collapse, that is, divergence of the displacement parameter. This principle may lead to some counterintuitive conclusions (the increase of the strength domain may destabilize a structural system (see Fig. 18), which is of course not true for a static system, described by classical limit analysis tools). It can be added at this stage that the influence of the mean force (drift term Δf_0) has already been quantified by Goodman in quasistatic analysis (see, for instance, [1]) in order to define a fatigue criterion. Authors think that such an additional term plays a crucial role for dynamic analysis as well. The symmetry property (especially the strength symmetry), concentrated into the parameter ϵ in the present study, has certainly to be taken into account, as an additional parameter, in the philosophy of seismic design.

IX. CONCLUSIONS

This paper is devoted to the stability and the dynamics of a harmonically excited damped elastic perfectly plastic asymmetrical oscillator. The hysteretical system is written as a nonsmooth forced system. It is shown that the dimension of the phase space can be reduced using adapted variables (elastic displacement and displacement rate). The forced vibrations of such an oscillator are treated by numerical approach by using the time locating techniques. The boundary between shakedown and dynamic ratcheting is obtained and is similar to the one of the symmetrical system. Periodic orbits with one plastic phase per cycle or two plastic phases per cycle are then analytically characterized. The stability of the limit cycles is analytically investigated with a perturbation approach. Finally, the rate of divergence (in the case of dynamic ratcheting) is corroborated to the asymmetric parameter. This means that the ratcheting divergence is more pronounced for a highly asymmetrical oscillator.

As a main lesson of such a constitutive model, one can keep in mind that the symmetric configuration is a stabilizing factor (symmetry of loading or symmetry of strength domain). On the contrary, asymmetrical configuration generally leads to dynamic ratcheting, or incremental collapse, that is, divergence of the displacement parameter. This principle may lead to some counterintuitive conclusions (the increase of the strength domain may destabilize a structural system, which is of course not true for a static system, described by classical limit analysis tools). The symmetry property, concentrated into the parameter ϵ in the present study, has certainly to be taken into account as an additional parameter in the philosophy of seismic design.

APPENDIX A: TIME CHARACTERISTICS OF THE (1,1) PERIODIC ORBIT

The system Eq. (31) characterizes the time parameters of the $(1,1)$ periodical solution,

$$\begin{vmatrix} \hat{A}\cos(\omega\tau_0) + \hat{B}\sin(\omega\tau_0) = \hat{C} \\ \hat{D}\cos(\omega\tau_0) + \hat{E}\sin(\omega\tau_0) = \hat{F} \end{vmatrix}, \text{ and } \bar{y} = \tau_1 - \tau_0. \quad (31')$$

The constants of system Eq. (31′), denoted by $\hat{A}$, $\hat{B}$, $\hat{C}$, $\hat{D}$, $\hat{E}$, and $\hat{F}$, are given below:

$$\hat{A} = \frac{f_0}{(1-\omega^2)^2 + 4\omega^2\zeta^2}\left[\begin{array}{l} -(1-\omega^2)e^{-\zeta\bar{y}}\cos(\sqrt{1-\zeta^2}\bar{y}) - \dfrac{\zeta}{\sqrt{1-\zeta^2}}(1+\omega^2)e^{-\zeta\bar{y}}\sin(\sqrt{1-\zeta^2}\bar{y}) \\ +(1-\omega^2)\cos(\omega\bar{y}) + 2\omega\zeta\sin(\omega\bar{y}) \end{array}\right] \quad (A1)$$

$$\hat{B} = \frac{f_0}{(1-\omega^2)^2 + 4\omega^2\zeta^2}\left[\begin{array}{l} -2\omega\zeta e^{-\zeta\bar{y}}\cos(\sqrt{1-\zeta^2}\bar{y}) + \dfrac{\omega(1-\omega^2-2\zeta^2)}{\sqrt{1-\zeta^2}}e^{-\zeta\bar{y}}\sin(\sqrt{1-\zeta^2}\bar{y}) \\ -(1-\omega^2)\sin(\omega\bar{y}) + 2\omega\zeta\cos(\omega\bar{y}) \end{array}\right] \quad (A2)$$

$$\hat{C} = 1 - e^{-\zeta\bar{y}}\cos(\sqrt{1-\zeta^2}\bar{y}) - \frac{\zeta}{\sqrt{1-\zeta^2}}e^{-\zeta\bar{y}}\sin(\sqrt{1-\zeta^2}\bar{y}) \quad (A3)$$

$$\hat{D} = -\frac{f_0}{4\zeta^2+\omega^2}\left\{-2\zeta + [2\zeta\cos(\omega\bar{y}) + \omega\sin(\omega\bar{y})]e^{-2\zeta\left(\frac{2\pi}{\omega}-\bar{y}\right)}\right\} + \frac{f_0 e^{-2\zeta\left(\frac{2\pi}{\omega}-\bar{y}\right)}}{(1-\omega^2)^2+4\omega^2\zeta^2}\begin{bmatrix} -2\omega^2\zeta e^{-\zeta\bar{y}}\cos\left(\sqrt{1-\zeta^2}\bar{y}\right) + \dfrac{2\omega^2\zeta^2+1-\omega^2}{\sqrt{1-\zeta^2}}e^{-\zeta\bar{y}}\sin(\sqrt{1-\zeta^2}\bar{y}) \\ +2\omega^2\zeta\cos(\omega\bar{y}) - \omega(1-\omega^2)\sin(\omega\bar{y}) \end{bmatrix} \tag{A4}$$

$$\hat{E} = -\frac{f_0}{4\zeta^2+\omega^2}\left\{-\omega + [\omega\cos(\omega\bar{y}) - 2\zeta\sin(\omega\bar{y})]e^{-2\zeta\left(\frac{2\pi}{\omega}-\bar{y}\right)}\right\} + \frac{f_0 e^{-2\zeta\left(\frac{2\pi}{\omega}-\bar{y}\right)}}{(1-\omega^2)^2+4\omega^2\zeta^2}\begin{bmatrix} \omega(1-\omega^2)e^{-\zeta\bar{y}}\cos(\sqrt{1-\zeta^2}\bar{y}) + \dfrac{\omega\zeta(1+\omega^2)}{\sqrt{1-\zeta^2}}e^{-\zeta\bar{y}}\sin(\sqrt{1-\zeta^2}\bar{y}) \\ -2\omega^2\zeta\sin(\omega\bar{y}) - \omega(1-\omega^2)\cos(\omega\bar{y}) \end{bmatrix} \tag{A5}$$

$$\hat{F} = \frac{1}{2\zeta}(1-e^{-2\zeta[(2\pi/\omega)-\bar{y}]}) + e^{-2\zeta[(2\pi/\omega)-\bar{y}]}\frac{\sin(\sqrt{1-\zeta^2}\bar{y})}{\sqrt{1-\zeta^2}} \tag{A6}$$

APPENDIX B: DETERMINATION OF THE COEFFICIENTS FOR THE STABILITY ANALYSIS – (1,1) PERIODIC ORBIT

The first coefficient to be determined is A_{11}, defined by,

$$\Delta\tau_1 = A_{11}\Delta\tau_0. \tag{B1}$$

In the elastic regime, evolution of v is given by Eq. (26), which can be written as

$$v(\tau_0,\tau) = e^{-\zeta(\tau-\tau_0)}\{A_1\cos[\sqrt{1-\zeta^2}(\tau-\tau_0)] + B_1\sin[\sqrt{1-\zeta^2}(\tau-\tau_0)]\} + C_1\cos\omega\tau + D_1\sin\omega\tau \quad \text{with} \quad \begin{vmatrix} A_1 = 1 - C_1\cos\omega\tau_0 - D_1\sin\omega\tau_0 \\ B_1 = \dfrac{A_1\zeta + C_1\omega\sin\omega\tau_0 - D_1\omega\cos\omega\tau_0}{\sqrt{1-\zeta^2}} \\ C_1 = f_0\dfrac{1-\omega^2}{(1-\omega^2)^2+4\omega^2\zeta^2} \\ D_1 = f_0\dfrac{2\zeta\omega}{(1-\omega^2)^2+4\omega^2\zeta^2} \end{vmatrix}. \tag{B2}$$

A perturbation approach is used

$$\begin{vmatrix} v(\tau_0,\tau_1) = 1 \\ v(\tau_0+\Delta\tau_0,\tau_1+\Delta\tau_1) = v(\tau_0,\tau_1) + \Delta\tau_0\dfrac{\partial v(\tau_0,\tau_1)}{\partial\tau_0} + \Delta\tau_1\dfrac{\partial v(\tau_0,\tau_1)}{\partial\tau_1} = 1 \end{vmatrix}. \tag{B3}$$

The second equation of (B3) leads to the determination of A_{11}

$$A_{11} = -\frac{\dfrac{\partial v(\tau_0,\tau_1)}{\partial\tau_0}}{\dfrac{\partial v(\tau_0,\tau_1)}{\partial\tau_1}}. \tag{B4}$$

A_{11} is finally calculated as

$$A_{11} = \frac{1-f_0\cos\omega\tau_0}{\dot{u}_1\sqrt{1-\zeta^2}}e^{-\zeta(\tau_1-\tau_0)}\sin[\sqrt{1-\zeta^2}(\tau_1-\tau_0)], \tag{B5}$$

where $\dot{u}_1$ is the displacement rate at the end of the elastic phase. $\dot{u}_1$ can be expressed by

$$\dot{u}_1 = e^{-\zeta(\tau_1-\tau_0)}\{(-\zeta A_1 + B_1\sqrt{1-\zeta^2})\cos[\sqrt{1-\zeta^2}(\tau_1-\tau_0)] + (-\zeta B_1 - A_1\sqrt{1-\zeta^2})\sin[\sqrt{1-\zeta^2}(\tau_1-\tau_0)]\} - C_1\omega\sin\omega\tau_1 + D_1\omega\cos\omega\tau_1. \tag{B6}$$

It is easy moreover to expand this term

$$\Delta\dot{u}_1 = \frac{\partial\dot{u}_1(\tau_0,\tau_1)}{\partial\tau_0}\Delta\tau_0 + \frac{\partial\dot{u}_1(\tau_0,\tau_1)}{\partial\tau_1}\Delta\tau_1. \tag{B7}$$

The term A_{31} can be deduced

$$A_{31} = \frac{\partial\dot{u}_1(\tau_0,\tau_1)}{\partial\tau_0} + A_{11}\frac{\partial\dot{u}_1(\tau_0,\tau_1)}{\partial\tau_1}. \tag{B8}$$

The terms of Eq. (B8) are detailed below:

$$\frac{\partial\dot{u}_1(\tau_0,\tau_1)}{\partial\tau_1} = -1 - 2\zeta\dot{u}_1 + f_0\cos\omega\tau_1 \tag{B9}$$

and

$$\frac{\partial\dot{u}_1(\tau_0,\tau_1)}{\partial\tau_0} = (1 - f_0\cos\omega\tau_0)e^{-\zeta(\tau_1-\tau_0)}\left\{\cos[\sqrt{1-\zeta^2}(\tau_1-\tau_0)] - \frac{\zeta}{\sqrt{1-\zeta^2}}\sin[\sqrt{1-\zeta^2}(\tau_1-\tau_0)]\right\} \tag{B10}$$

The same reasoning can be applied to the determination of B_{11} and B_{13}, obtained from the function $\dot{u}_2(\dot{u}_1,\tau_1,\tau_2)$

$$\dot{u}_2(\dot{u}_1,\tau_1,\tau_2) = B_2 e^{-2\zeta(\tau_2-\tau_1)} + C_2\cos\omega\tau_2 + D_2\sin\omega\tau_2 - \frac{1}{2\zeta}, \quad \text{with} \quad \left|\begin{array}{l} C_2 = f_0\dfrac{2\zeta}{\omega^2+4\zeta^2} \\ D_2 = f_0\dfrac{\omega}{\omega^2+4\zeta^2} \\ B_2 = \dot{u}_1 + \dfrac{1}{2\zeta} - C_2\cos\omega\tau_1 - D_2\sin\omega\tau_1 \end{array}\right. . \tag{B11}$$

The perturbation approach leads to

$$B_{11} = -\frac{\dfrac{\partial\dot{u}_2(\dot{u}_1,\tau_1,\tau_2)}{\partial\tau_1}}{\dfrac{\partial\dot{u}_2(\dot{u}_1,\tau_1,\tau_2)}{\partial\tau_2}} \quad \text{and} \quad B_{13} = -\frac{\dfrac{\partial\dot{u}_2(\dot{u}_1,\tau_1,\tau_2)}{\partial\dot{u}_1}}{\dfrac{\partial\dot{u}_2(\dot{u}_1,\tau_1,\tau_2)}{\partial\tau_2}}. \tag{B12}$$

These terms are calculated as following

$$B_{11} = \frac{e^{-2\zeta(\tau_2-\tau_1)}}{1 - f_0\cos\omega\tau_0}(1 + 2\zeta\dot{u}_1 - f_0\cos\omega\tau_1) \tag{B13}$$

and

$$B_{13} = \frac{e^{-2\zeta(\tau_2-\tau_1)}}{1 - f_0\cos\omega\tau_0}.$$

Some simplification occurs by noticing that

$$B_{11} = -B_{13}\frac{\partial\dot{u}_1(\tau_0,\tau_1)}{\partial\tau_1}. \tag{B14}$$

R is then simplified by

$$R = B_{13}\frac{\partial\dot{u}_1(\tau_0,\tau_1)}{\partial\tau_0} = e^{-\zeta\left(\tau_0-\tau_1+\frac{4\pi}{\omega}\right)}\left\{\cos\left[\sqrt{1-\zeta^2}(\tau_1-\tau_0)\right] - \frac{\zeta}{\sqrt{1-\zeta^2}}\sin[\sqrt{1-\zeta^2}(\tau_1-\tau_0)]\right\}. \tag{B15}$$

APPENDIX C: DETERMINATION OF THE COEFFICIENTS FOR THE STABILITY ANALYSIS – (1,2) PERIODIC ORBIT

As in Appendix B, the first coefficient to be determined is A'_{11} defined by

$$\Delta\tau_1 = A'_{11}\Delta\tau_0 \quad \text{with } A'_{11} = -\frac{\dfrac{\partial v(\tau_0,\tau_1)}{\partial\tau_0}}{\dfrac{\partial v(\tau_0,\tau_1)}{\partial\tau_1}}. \tag{C1}$$

A'_{11} is finally calculated as

$$A'_{11} = \frac{(1+\varepsilon) + f_0 \cos \omega\tau_0}{\dot{u}_1\sqrt{1-\zeta^2}} e^{-\zeta(\tau_1-\tau_0)} \sin[\sqrt{1-\zeta^2}(\tau_1-\tau_0)], \tag{C2}$$

where $\dot{u}_1$ is the displacement rate at the end of the elastic phase.

The term A'_{31} can be deduced from

$$A'_{31} = \frac{\partial \dot{u}_1(\tau_0,\tau_1)}{\partial\tau_0} + A'_{11}\frac{\partial \dot{u}_1(\tau_0,\tau_1)}{\partial\tau_1}. \tag{C3}$$

The terms of Eq. (C3) are detailed below:

$$\frac{\partial \dot{u}_1(\tau_0,\tau_1)}{\partial\tau_1} = -1 - 2\zeta\dot{u}_1 + f_0 \cos \omega\tau_1 \tag{C4}$$

and

$$\frac{\partial \dot{u}_1(\tau_0,\tau_1)}{\partial\tau_0} = [(1+\varepsilon) + f_0 \cos \omega\tau_0] e^{-\zeta(\tau_1-\tau_0)} \left\{ -\cos\left[\sqrt{1-\zeta^2}(\tau_1 - \tau_0)\right] + \frac{\zeta}{\sqrt{1-\zeta^2}} \sin[\sqrt{1-\zeta^2}(\tau_1-\tau_0)] \right\} \tag{C5}$$

The same reasoning can be applied to the determination of B'_{11} and B'_{13}, obtained from the function $\dot{u}_2(\dot{u}_1, \tau_1, \tau_2)$.

$$B'_{11} = -\frac{\dfrac{\partial \dot{u}_2(\dot{u}_1,\tau_1,\tau_2)}{\partial\tau_1}}{\dfrac{\partial \dot{u}_2(\dot{u}_1,\tau_1,\tau_2)}{\partial\tau_2}} \quad \text{and} \quad B'_{13} = -\frac{\dfrac{\partial \dot{u}_2(\dot{u}_1,\tau_1,\tau_2)}{\partial\dot{u}_1}}{\dfrac{\partial \dot{u}_2(\dot{u}_1,\tau_1,\tau_2)}{\partial\tau_2}} \tag{C6}$$

These terms are calculated as following

$$B'_{11} = \frac{e^{-2\zeta(\tau_2-\tau_1)}}{1 - f_0 \cos \omega\tau_2}(1 + 2\zeta\dot{u}_1 - f_0 \cos \omega\tau_1) \tag{C7}$$

and

$$B'_{13} = \frac{e^{-2\zeta(\tau_2-\tau_1)}}{1 - f_0 \cos \omega\tau_2}.$$

R' is calculated from

$$R' = B'_{11}A'_{11} + B'_{13}A'_{31}. \tag{C8}$$

Equation (C8) is detailed below:

$$R' = e^{-2\zeta(\tau_2-\tau_1)} e^{-\zeta(\tau_1-\tau_0)} \frac{(1+\varepsilon) + f_0 \cos \omega\tau_0}{1 - f_0 \cos \omega\tau_2} \left\{ -\cos[\sqrt{1-\zeta^2}(\tau_1 - \tau_0)] + \frac{\zeta}{\sqrt{1-\zeta^2}} \sin[\sqrt{1-\zeta^2}(\tau_1-\tau_0)] \right\}. \tag{C9}$$

The particular case of $\varepsilon=0$ and $\tau_2=\tau_0+(\pi/\omega)$ leads to the following value of R' (symmetrical case [31]):

$$R' = e^{-\zeta\left(\tau_0-\tau_1+\frac{2\pi}{\omega}\right)} \left\{ -\cos[\sqrt{1-\zeta^2}(\tau_1-\tau_0)] + \frac{\zeta}{\sqrt{1-\zeta^2}} \sin[\sqrt{1-\zeta^2}(\tau_1-\tau_0)] \right\}. \tag{C10}$$

The calculation of R'' is similar to the one of R', given in Eq. (C9)

$$R'' = e^{-2\zeta(\tau_4-\tau_3)} e^{-\zeta(\tau_3-\tau_2)} \frac{1 - f_0 \cos \omega\tau_2}{(1+\varepsilon) + f_0 \cos \omega\tau_4} \times \left\{ -\cos[\sqrt{1-\zeta^2}(\tau_3-\tau_2)] + \frac{\zeta}{\sqrt{1-\zeta^2}} \times \sin[\sqrt{1-\zeta^2}(\tau_3-\tau_2)] \right\}. \tag{C11}$$

For the same reasons, the particular case of $\varepsilon=0$ leads to the simple result

$$R'' = R'. \tag{C12}$$

Finally, in the general case ($\varepsilon \neq 0$), the amplification factor R ($R=R'R''$) is equal to

$$R = e^{-2\zeta(\tau_4-\tau_3+\tau_2-\tau_1)} e^{-\zeta(\tau_3-\tau_2+\tau_1-\tau_0)} \left\{ -\cos[\sqrt{1-\zeta^2}(\tau_3-\tau_2)] + \frac{\zeta}{\sqrt{1-\zeta^2}} \sin[\sqrt{1-\zeta^2}(\tau_3-\tau_2)] \right\} \left\{ -\cos[\sqrt{1-\zeta^2}(\tau_1-\tau_0)] + \frac{\zeta}{\sqrt{1-\zeta^2}} \sin[\sqrt{1-\zeta^2}(\tau_1-\tau_0)] \right\}. \tag{C13}$$

[1] J. Lemaitre and J. L. Chaboche, *Mechanics of Solid Materials* (Cambridge University Press, Cambridge, 1990).
[2] J. L. Chaboche, Eur. J. Mech. A/Solids **13**, 501 (1994).
[3] R. P. Feynman, R. B. Leighton, and M. Sands, *The Feynman Lectures on Physics* (Addison-Wesley, Reading, MA, 1966), Vol. 1, Chap. 46.
[4] A. Ajdari and J. Prost, C. R. Acad. Sci., Ser. II: Mec., Phys., Chim., Sci. Terre Univers **315**, 1635 (1992).
[5] F. Jülicher, A. Adjari, and J. Prost, Rev. Mod. Phys. **69**, 1269 (1997).
[6] S. Flach, O. Yevtushenko, and Y. Zolotaryuk, Phys. Rev. Lett. **84**, 2358 (2002).
[7] M. Barbi and M. Salerno, Phys. Rev. E **62**, 1988 (2000).
[8] B. Norden, Y. Zolotaryuk, P. L. Christiansen, and A. V. Zolotaryuk, Phys. Rev. E **65**, 011110 (2001).
[9] P. Reimann, Phys. Rev. Lett. **86**, 4992 (2001).
[10] P. Reimann, Phys. Rep. **361**, 57 (2002).
[11] E. Pavlovskaia and M. Wiercigroch, Phys. Rev. E **64**, 056224 (2001).
[12] I. S. Ahn, S. S. Chen, and G. F. Dargush, J. Eng. Mech. **132**, 411 (2006).
[13] M. Jirasek and Z. P. Bazant, *Inelastic Analysis of Structures*

(Wiley, Chichester, 2002).
[14] J. Awrejcewicz and C. H. Lamarque, *Bifurcations and Chaos in Nonsmooth Mechanical Systems* (World Scientific, Singapore, 2003).
[15] L. S. Jacobsen, in *Symposium Earthquake and Blast Effects on Structures* (1952), pp. 94–113.
[16] R. Tanabashi, in *Proceedings of the World Conference on Earthquake Engineering*, Berkeley, CA (1956), 6-1-6-7.
[17] T. K. Caughey, J. Appl. Mech. **27**, 649 (1960).
[18] P. C. Jennings, J. Eng. Mech. **90**, 131 (1964).
[19] W. D. Iwan, J. Appl. Mech. **32**, 921 (1965).
[20] D. Capecchi, Dyn. Stab. Syst. **6**(2), 89 (1991).
[21] D. Capecchi and F. Vestroni, Int. J. Non-Linear Mech. **25**(2-3), 309 (1990).
[22] S. Chatterjee, A. K. Mallik, and A. Ghosh, J. Sound Vib. **191**(1), 129 (1996).
[23] S. F. Masri, J. Acoust. Soc. Am. **47**, 229 (1970).
[24] S. F. Masri and T. K. Caughey, J. Appl. Mech. **33**, 586 (1966).
[25] G. R. Miller and M. E. Butler, J. Eng. Mech. **114**(3), 536 (1988).
[26] D. Capecchi, Int. J. Non-Linear Mech. **30**(23), 3303 (1993).
[27] S. F. Masri, J. Acoust. Soc. Am. **57**, 105 (1975).
[28] W. D. Iwan, in *Proceedings the Third World Conference Earthquake Engineering* (1964).
[29] C. D. Coman, Discrete Contin. Dyn. Syst., Ser. B **3**(2), 163 (2003).
[30] C. S. Liu and Z. M. Huang, J. Sound Vib. **273**, 149 (2004).
[31] N. Challamel and G. Gilles, J. Sound Vib. **301**, 608 (2007).
[32] J. Song and A. der Kiureghian, J. Eng. Mech. **132**(6), 610 (2006).
[33] L. S. Jacobsen, Trans. ASME **52**, 15 (1930).
[34] J. P. Den Hartog, Trans. ASME **53**, 107 (1931).
[35] J. P. Den Hartog and S. J. Mikina, Trans. ASME **54**, 157 (1932).
[36] M. Wiercigroch and Chaos, Chaos, Solitons Fractals **11**, 2429 (2000).
[37] J. C. Ji and A. Y. T. Leung, Int. J. Mech. Sci. **46**, 1807 (2004).
[38] A. C. J. Luo and L. Chen, Chaos, Solitons Fractals **24**, 567 (2005).
[39] G. Csernak and G. Stépàn, J. Sound Vib. **295**, 649 (2006).
[40] D. J. Wagg, Chaos, Solitons Fractals **16**, 779 (2003).
[41] N. Challamel, Int. J. Struct. Stab. Dyn. **5**(2), 259 (2005).
[42] S. W. Shaw and P. J. Holmes, J. Sound Vib. **90**, 129 (1983).